HYDROLOGICAL PROCESSES
Hydrol. Process. (2015)
Published online in Wiley Online Library
(wileyonlinelibrary.com) DOI: 10.1002/hyp.10438

Hydropeaking induces losses from a river reach: observations at multiple spatial scales

B. Yellen* and D.F. Boutt

Department of Geosciences, University of Massachusetts, Amherst, MA 01003, USA

Abstract:

In humid regions, where gaining river conditions generally prevail, daily hydroelectric dam releases alter downstream surface water–groundwater interactions by reversing the head gradient between river and adjacent groundwater. Previously, it has been noted that artificial stage changes due to dam releases enhance hyporheic exchange. Here we investigate the regulated Deerfield River in northwestern Massachusetts at multiple scales to evaluate how changing downstream geologic conditions along the river mediate this artificial hyporheic pumping.

Water budget analysis indicates that roughly 10% of bank-stored water is permanently lost from the 19.5-km river reach, likely as a result of transpiration by bank vegetation. An adjacent reference stream with similar dimensions and geomorphology, but without hydropeaking, shows predictable gaining conditions. Field observations from streambed piezometers and thermistors show that water losses are not uniform throughout the study reach. Riparian aquifer transmissivity in river sub-reaches largely determines the magnitude of surface water–groundwater exchange as well as net water loss from the river. These newly documented losses from hydropeaking river systems should inform decisions by river managers and hydroelectric operators of additional tradeoffs of oscillatory dam-release river management. Copyright © 2015 John Wiley & Sons, Ltd.

KEY WORDS hyporheic; hydropeaking; dam release; surface water-groundwater; Deerfield River; streambed temperature

Received 4 June 2014; Accepted 20 January 2015

INTRODUCTION

For several decades, river and wetland ecologists have documented and publicized the impacts of dams on fish and other biota (e.g. Raymond, 1979; Ward and Stanford, 1983; Poff *et al.*, 1997). In addition to impacting flow regime and geomorphic processes (e.g. Ligon *et al.*, 1995; Magilligan *et al.,* 2003), hydrologists have recently recognized the potential for abrupt, anthropogenic stage changes downstream from hydroelectric dams to dramatically alter surface water–groundwater (SWGW) interactions (Arntzen *et al.*, 2006; Boutt and Fleming, 2009; Sawyer *et al.*, 2009). Whereas most river reaches consistently gain or lose water, particularly within a given season, dam-controlled rivers often switch from gaining to losing on the time scale of daily energy demand cycles. Hydropeaking—discrete dam releases during periods of peak electricity demand—raises and lowers river stage abruptly. Downstream from hydropeaking dams, abrupt stage changes reverse the vertical head gradient (VHG) between surface water and underlying groundwater, thus causing these reaches to continually alternate between gaining and losing states.

In the last twenty five years, several investigators have documented crucial stream processes at work within the hyporheic zone (Boulton *et. al*, 2010), the region below a stream where stream and ground water mix (Brunke and Gonser, 1997). These processes include mediation of cycling of nitrogen (Jones *et al.*, 1995), phosphorous (Mullholland *et al.*, 1997), and carbon (Findlay *et al.*, 1993) within streams. Recent recognition of the importance of hyporheic zone processes to river ecosystems coupled with the near ubiquity of flow alteration in the developed world (Graf, 1999) makes it essential that we understand how hydropeaking may be altering SWGW interactions and the sensitive ecotone that inhabits streambeds. Here, we explore how changing downstream geologic conditions shape the magnitude and direction of changes in the hyporheic zone associated with hydropeaking. Furthermore, we propose that in certain conditions, hydropeaking can cause a typically gaining river reach to permanently lose water.

A handful of studies have used streambed probes, often at a single study site, to make discrete measurements to document alterations to SWGW interactions as a result of hydropeaking. Arntzen *et al.* (2006) noted a hysteretic pattern of VHG reversals in riverbed materials in the

*Correspondence to: Yellen B., Department of Geosciences, University of Massachusetts, Amherst, MA 01003, USA.
E-mail: byellen@geo.umass.edu

Hanford Reach of the Columbia River downstream of a dam with ~2-m stage changes. Most notably, variation in the magnitude of the VHG at different sites was largely a product of different bed material conductivity. Sawyer *et al*. (2009) extensively documented the altered SWGW exchange dynamics at a study site downstream from Austin, Texas, USA on the Colorado River. The authors used piezometric data, geochemical observations, and heat tracer data to illustrate how hydropeaking causes a dramatic increase in the extent of the hyporheic zone (HZ) at the study site. At the same site, Gerecht *et al.* (2011) noted the potential for hyporheic pumping to impact streambed temperature and provide thermal buffering at low stage when the river quickly reclaimed water from the overpressured streambed. Hanrahan (2008) monitored VHG at sites of known importance for salmon spawning in a mostly bedrock-bound reach of the Snake River. From observations of minimal VHG despite large, abrupt stage changes, he concluded that dam-induced hyporheic exchange was minimal due to limited unconsolidated bank material in the canyon setting of the study site. All of these studies evaluated the phenomenon of hydropeaking-induced SWGW exchange as a function of very local site properties. Here, we build on their work by investigating this phenomenon at larger spatial scales, incorporating water budget analysis and the potential impact of reach geomorphology on hyporheic pumping.

On the Deerfield River in western Massachusetts, we set out to better understand the effect of reach-scale geologic characteristics, such as changing valley aquifer morphology and stratigraphy, on the magnitude and direction of dam-induced hyporheic exchange. Indication that the study reach loses water, despite its location within the humid northeastern United States, led us to focus on the role of dam-control in potentially causing rivers to lose water. Whereas previous studies have focused on a single site or small collection of sites, we use a combination of discrete scale field measurements as well as reach-scale water budget analysis to obtain a more systemic picture of the effects of abrupt stage changes on SWGW interactions. Furthermore, we focus on the role of riparian aquifer characteristics, including hydraulic properties and variation in areal extent, in controlling the nature of dam-induced SWGW intermixing.

SITE DESCRIPTION

The Deerfield River (DFR) watershed covers 1722 km^2 across portions of southern Vermont and northwestern Massachusetts, USA before entering the Connecticut River in Greenfield, Massachusetts (Figure 1A). Our study reach stretches from the Fife Brook Dam in Rowe,

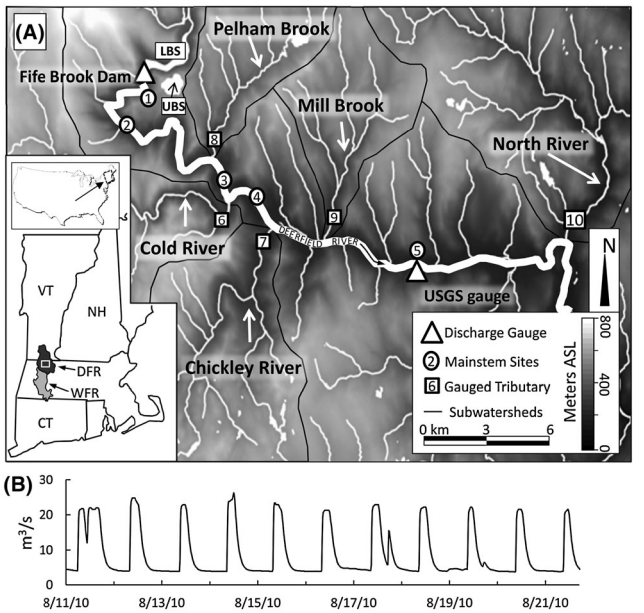

Figure 1. (A) Site map of the study area. The entire DFR watershed is shown in inset at bottom left spanning parts of Vermont and Massachusetts. The WFR watershed is just south of DFR. In the shaded elevation map, the mainstem of the DFR (thick white line) runs southeastward with the study reach defined by the two discharge sites (triangles). The Lower Bear Swamp (LBS) impoundment and Upper Bear Swamp (UBS) pump-storage reservoir appear in the northwest corner of the blown up area. Four large tributaries within the study reach, as well as North River are labeled. (B) Typical summer discharge fluctuations on the Deerfield River during a 10-day dry period

MA 19.5 km downstream to USGS gaging station 01168500 in Charlemont, MA. In the span of the study reach, tributaries and streams entering the DFR increase the river's contributing area 40.4% from 666 km^2 at the upstream end of the reach to 935 km^2 downstream. In this reach, four major subwatersheds (area $>$ 30 km^2 each) enter the DFR, accounting for roughly 80% of the increase in contributing area.

The largely rural watershed (>90% forested) displays typical Northeastern United States climate throughout most of its area. Average annual precipitation reported by gauges within the watershed ranges from 110 to 130 cm depending on elevation. Precipitation is distributed evenly among the seasons. Seasonal variations in evapotranspiration play a dominant role in controlling average monthly runoff, with a disproportionate amount of runoff occurring during spring due to snow melt and high soil moisture conditions.

A steep longitudinal river gradient (slope = 0.075 in dammed reach) and humid climate make the DFR ideal for hydroelectric power generation. Harriman and Somerset reservoirs (off north edge of Figure 1A) in the Vermont part of the watershed provide most of the storage for six downstream run-of-river generating facilities by storing on average 54% of mean annual discharge. These large upstream reservoirs are drawn

down in late winter (see Supplementary Figure 1), providing storage for flood control during the spring freshet and power generation as the stored spring floods are incrementally released during summer peaks in energy demand (P. Moriarty, personal communication, November 30, 2010). Storage of the spring flood suppresses the annual hydrograph, largely preventing discharge events greater than 400 m^3/s within the study reach.

The summer hydrograph within the study reach is dominated by the signature of Fife Brook Dam, a small impoundment (low flow residence time < 3 days) constructed in 1974 that allows for hydropeaking and provides water for pump storage generation. On an average summer day, discharge from the dam increases from 3.5 m^3/s to 25 m^3/s for roughly 8 midday hours, raising river stage anywhere from 0.4 to 0.7 m depending on channel morphology (Figure 1B.).

The study reach is located in the Berkshire Hills physiographic province (Friesz, 1996), characterized by narrow river valleys surrounded by steep bedrock hill slopes. Lower gradient valley bottoms generally contain 0–20 m stratified drift and modern alluvium. However, in some locations Pleistocene glaciation over-deepened a few bedrock valleys, which now accommodate up to 50 m of this unconsolidated material in places. We refer to this valley fill material that is hydraulically connected to a local drain as the riparian aquifer. The majority (70%) of riparian groundwater basin recharge is derived from adjacent metamorphic crystalline bedrock uplands via runoff, fracture flow and shallow subsurface flow (Friesz, 1996). Other recharge occurs via direct precipitation inputs to water bodies and tributary valley bottoms.

Along the study reach, riparian aquifer hydraulic conductivities change dramatically. The upper 5.5 km of the reach is largely bedrock-bound, with the exception of a ~7-m depth to bedrock observed at site 2. Mabee *et al.* (2007) detailed the extent and nature of the valley fill aquifer spanning the lower 14 km of the study reach. Strata there are typical of glacial morphosequence valleys (Koteff and Pessl, 1981): fining upwards glaciofluvial deposits throughout the site with glaciolacustrine sediment overlying the most downstream parts of the reach in Charlemont, MA (Figure 2). Reworking of coarse proglacial delta sediments has mantled the modern valley bottom with high conductivity (30–100 m/d) modern alluvium. As glacial lakes drained and the valley adjusted to lowered base level, the mainstem of the river has incised through this surface alluvium in most locations and the streambed directly overlies glaciofluvial sediments. Streambeds on the DFR and major tributaries are generally made up of cobbles and boulders that are only mobilized during high-discharge events. At pinch points

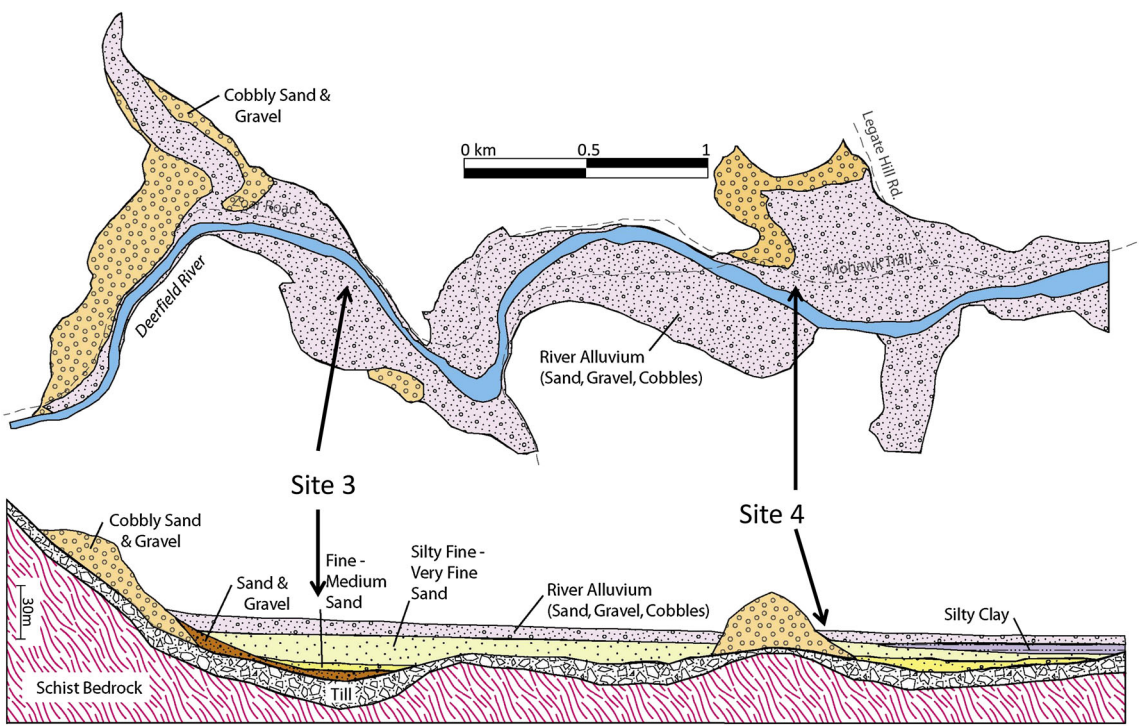

Figure 2. Map view (top) and cross section down the valley axis (bottom) of surficial geology of the lower two thirds of the study reach showing the glaciofluvial and glaciolacustrine deposits that fill the over-deepened bedrock valley (modified from Boutt 2010). The locations of sites 3 and 4 are indicated by black arrows on both the map and cross-section views. Sites 1 and 2 are upstream of this schematic. Site 5 and the downstream discharge gauge are just off the right side of this diagram

in the upper half of the study reach (such as site 1), where resistant bedrock outcrops along the banks, residue on extracted in-stream piezometers made up of a clay-rich matrix with angular grains embedded indicated that the river likely runs directly over lodgement till in these areas. At the most down-stream sections of the reach, the riverbed lies directly atop fine grained, low-permeability glaciolacustrine material.

Directly to the south of the DFR watershed, a series of gauges on the geomorphically similar Westfield River (WFR) allows for reliable comparison of SWGW processes in a reference watershed that lacks hydropeaking. The reach between upstream and down-stream discharge gauges measures approximately 28 km, the upper 13 km of which are relatively bound by bedrock. The lower 15 km of this reference reach flows through a broad alluvial valley similar to that of the lower Deerfield study reach. Flood control dams on two of the three WFR branches dampen annual peak flows, but generally do not modify seasonal median discharge as observed in the DFR.

METHODS

Water budget observations

We constructed a simple water budget to evaluate reach-scale SWGW interactions by accounting for major inputs to and outputs from the river system, excluding groundwater. Any difference in absolute value between system inputs and outputs therefore indicates gains from or losses to the riparian aquifer. There is no major groundwater or surface water withdrawal within this rural, mountainous watershed.

Upstream discharge from Fife Brook hydroelectric dam plus contributions of four major tributaries comprised water budget inputs. The four gauged tributaries cumulatively make up 80% of downstream increase in contributing area, thereby providing a minimum bound for surface water inputs. Evaporation plus downstream discharge measured at the Charlemont, Massachusetts USGS gauge (01168500) comprised outputs from the system. We estimated an evaporation time series using an energy balance approach according to Valiantzas (2006), which approximates the Penman Equation (Penman, 1948), but makes use of more commonly observed meteorological data. This method is a physically based energy balance approach that sums estimates of incoming short wave radiation, outgoing long wave radiation, and turbulent energy exchanges. Estimated linear evaporation rates were multiplied by the approximate surface area of the river reach to obtain a time series of volumetric losses from the river due to direct evaporation from the river surface. Thus, the water budget equation used was

$$GW = (Q_{dn} + E)\text{-}\left(Q_{up} + Q_{trib}\right) \quad (1)$$

where Q_{up} is discharge just downstream of the Fife Brook dam, Q_{trib} is the combined discharge of the four largest tributaries in the reach, Q_{dn} is discharge at the downstream end of the reach, and E is direct evaporation from the surface of the DFR. The difference between inputs and outputs—GW—represents changes in storage of the groundwater system. The two terms on the right side of Equation (1) are reversed from general convention in order that negative GW values indicate times when the river was losing water to the groundwater system. Positive values conversely indicate gaining conditions.

Continuous rain-free periods of nine days were identified during the summers of 2005 and 2010 for which we had reliable data to account for water budget inputs (Table I). Most of the data presented were collected during the summer of 2010. However, we also calculated the water budget during the summer of 2005, both because it was the only other summer for which Q_{up} data were available and to allow for comparison with other years to evaluate if patterns were consistent across multiple summers. In addition to summer analysis periods, two suitable periods for analysis were identified during spring and fall dormant conditions (shaded in Table I).

To account for flood wave travel time, each component of the water budget was lagged forward to correspond

Table I. Average values of water budget components for rain-free 9-day periods with associated error estimates for each integration. Dormant season reference time periods are shaded grey. GW indicates the net result of water budget calculations showing losses across all summer observation periods

	GW (m^3/s)	Qdn (m^3/s)	Qup (m^3/s)	Qtrib (m^3/s)	Avg E (m^3/s)
July 1–9, 2010	−0.99 ± 0.061	13.27 ± 0.002	13.75	0.64 ± 0.147	0.117 ± 0.001
Aug 8–16, 2010	−1.33 ± 0.134	12.10 ± 0.017	12.94	0.57 ± 0.103	0.075 ± 0.015
Sep 4–12, 2010	−0.93 ± 0.138	6.39 ± 0.007	6.75	0.65 ± 0.113	0.085 ± 0.017
Jul 22–30, 2005	−1.95 ± 0.414	8.51 ± 0.027	8.62	1.94 ± 0.384	0.094 ± 0.018
Aug 5–13, 2005	−1.52 ± 0.257	8.38 ± 0.470	8.85	1.13 ± 0.225	0.083 ± 0.017
Mar 20–28, 2005	3.79 ± 2.76	18.00 ± 2.28	11.38	3.59 ± 0.72	0.023 ± 0.001
Nov 7–13, 2009	−0.08 ± 5.48	24.1 ± 4.81	20.84	3.33 ± 0.67	0.012 ± 0.002

with earlier Q_{up} time stamps. Q_{dn} was lagged earlier by 4.5 h, which corresponded to the average time it took a 25 m^3/s pulse to travel the reach. E and Q_{trib} were each lagged 2.25 h to provide average parameter values during a given flood wave.

In order to evaluate the extent that different variables drive the system, individual dam-release events were delineated. Each event's beginning and end were denoted by departure from and subsequent return to minimum baseflow releases from Fife Brook Dam (Supplementary Figure 2A). Water budget time series components were integrated over given release events and summed to evaluate the extent of SWGW exchange for individual dam hydrographs. In this way, data points could be resolved from the various time series described in Equation (1). By calculating loss during each dam release, these data can be compared to potential causal mechanisms for river losses.

We tested the sensitivity of water budget results to varying lag times of Q_{dn} behind Q_{up}. Lag times were adjusted in half our increments from 3 h to 5.5 h. For each lag trial, the GW term was computed for several individual dam hydrographs and for 2010 9-day summation periods. Lags between 3 and 5-h tests show little change in net loss at daily or 9-day time scales, with an average change in the value of GW of 0.89% for all time periods tested (Supplementary Figure 2B). Because, observed lag times for flood propagation between gauges were consistent across analytical periods, and always between 4.25 and 4.75 h, we kept lags constant across analytical periods.

In order to perform calculations on 2005 data, a Q_{trib} record was reconstructed based on a linear regression between observed Q_{trib} values and those from the neighbouring North River, which has a USGS discharge gauge. Simulated 2010 Q_{trib} baseflow values at each time step differed from the observed time series by an average of 3%. The small total discharge of the four tributaries relative to that of the DFR study reach causes this error to be less than 1% of the GW term for 2005 analytical periods.

A simpler water budget was constructed for the adjacent Westfield River (WFR) that accounts for only upstream and downstream discharge. Tributary inputs were not available for this system. Upstream discharge data were compiled by adding values from a gauge on each of the WFR's three main branches (USGS gauges 0118100, 01180500, and 01179500). Downstream discharge is taken from a USGS gauge (01183500) located 28 km downstream of the confluence of the three branches.

Error propagation

Using conservative values of each water budget component in order to minimize estimated losses from the river, we tested whether perceived losing conditions could be due simply to observational error. To do this, we considered maximum possible outputs from the system and minimum adjusted inputs. Q_{dn} was adjusted higher by a constant percentage corresponding to the average of the absolute value of error reported from USGS field measurements at the site. This reported error is the percent difference between observed discharge and that inferred from the stage. Where the specific field measurements following evaluation periods used to make error adjustments, Q_{dn} would have been revised smaller, and thereby driven losses more negative, defeating the stated goal of this loss minimization exercise. Instead we averaged the absolute value of all field measurements ($n = 68$) dating back to 1948 on days when discharge was less than 30 m^3/s. There was no relationship between discharge and measurement error. To adjust the Q_{dn} record, each observation in the time series was adjusted upwards by 0.13%, which corresponded to the average error in the historic records.

To conservatively evaluate error in Q_{trib}, we subtracted 20% from each observation, consistent with minimizing losses from the river. Q_t only considers discharge from four tributaries and does not account for surface water inputs from 20% of the reach catchment made up of smaller streams. Therefore, Q_t adjusted with this error is almost certainly lower than actual tributary inputs, thereby avoiding possibility of overestimating losses from the river. Observations from the E time series were also each revised upwards by 20%, bringing average E consistently above regional daily evaporation estimates reported in the region. Q_{up} was measured by utility companies and verified via independent observations of dam tailwater stage coupled with a rating curve and electrical power production. Due to the rigor applied and the multiple measurement methods, we have not adjusted Q_{up} in error analysis.

Streambed observations

Five study sites within the 19.5-km study reach were instrumented to collect discrete measurements of VHG and streambed temperatures. We selected field sites to capture a range of riparian aquifer geometries, from bedrock bound channel at site 1, to extensive stratified drift at sites 3 and 4, and intermediary conditions at sites 2 and 5. At sites 1 and 2, we performed seismic refraction surveys and pinned the bedrock reflector to the bottom of a schematic glacial U-shaped valley. At sites 3 and 4, extensive borehole and geophysical investigations detailed in Mabee *et al.* (2007) were used to constrain aquifer geometry.

Streambed head and river stage were used to calculate vertical hydraulic gradient (VHG) as the ratio of the

difference in head between the river and the underlying groundwater over the distance between the river bottom and the top of the piezometer screen following Arntzen *et al.* (2006):

$$VHG = \frac{h_{HZ} - h_R}{z_R - z_S} \quad (2)$$

where h_{HZ} and h_R are head in the hyporheic zone and river, respectively; z_R and z_S are elevation above an arbitrary datum of the river bottom and the top of the well screen, respectively. Thus, when the numerator is positive, head in the streambed exceeds that in the river and we assume that the river gains water from the aquifer.

At each site, VHG and vertical temperature distribution were monitored. Limited equipment precluded simultaneous monitoring at all sites. Between two and five days of observations were recorded at each site during periods of non-precipitation and routine hydropeaking (e.g. Figure 1A). Each monitoring deployment captured at least two dam-induced floods, ensuring that we captured changes in the direction of the hydraulic gradient. Streambed VHG and temperature observations were collected from 4-cm outside-diameter solid steel pipes following the recommendations of Cardenas (2010) fitted to a drive point. We screened piezometers by drilling six 1-cm perforations 10 cm above the drive point. Piezometers were deployed at ~10-cm river depth during low stage by driving with a slide sledge until the top of the screen was 50 cm below the streambed, after which the piezometer was developed by flushing the screen with approximately 10 l of water. Pressure transducer data loggers (Solinst LevelLoger 3001, 1.4-mm resolution) were placed in these piezometers and in the river to record river stage and hyporheic zone head at 5-min intervals. Temperature loggers (iButton model DS1921Z, 0.125 °C resolution) were placed in similarly constructed piezometers affixed to a metal rod to measure temperature in the river and the streambed at 10 cm and 30 cm below the river bottom. Rubber baffles inside the piezometer every 10 cm limited convective heat transport within the well. The VTD probe at site 3 malfunctioned. As a substitute, we make use of temperature data from the VHG pressure transducer pair, which record temperature in addition to absolute pressure. The HZ pressure transducer was at a depth of 50 cm, 20 cm below the lowest thermistors at other sites.

In addition to monitoring VHG, we conducted slug tests to estimate bed hydraulic conductivity prior to removal of each streambed piezometer. Wells were redeveloped by pouring roughly 10 l of river water into the pipe and allowing time for the head to return to static level. A 50-cm section of pipe fitted with a false bottom and filled with river water was used to instantaneously raise the head in the well. A pressure transducer recorded the head recovery at 1-s intervals. The recovery was modeled using Bouwer–Rice method (Bouwer and Rice, 1976), which is appropriate for underdamped systems where the well screen is completely within the saturated zone. Three slug tests were performed for each piezometer. Due to problems with short circuiting around the outside of the well bore immediately after piezometer emplacement, we could only perform slug tests on our wells that had been deployed for several days and subsequently redeveloped. Thus, only one well could be tested at each of the five study sites.

Riparian aquifer wells

We make use of data collected previously as part of a study of groundwater resources within the region (Friesz, 1996). Two wells were installed at distances of 3 m and 40 m from the river at site 4 (see Figure 1A for location), where the river flows through a broad alluvial aquifer. Both wells were screened in coarse alluvium. River stage oscillations propagate through the conductive alluvial sediments there and are evident in both well hydrographs. We use the horizontal distance between these wells and the difference in head during summer of 1994 to calculate a time series of hydraulic gradient within the riparian aquifer. This gradient time series, coupled with Friesz's (1996) estimate of hydraulic conductivity of 100 m/d was used to calculate a Darcy-based horizontal flux adjacent to the river.

RESULTS

Water budget calculations

Water budgeting indicates that the DFR study reach consistently lost water to the adjacent aquifer over 24-h periods during summer months. Several nine day summations of the GW term in Equation (1) across two water years all show water losses (negative GW terms) from the river to the riparian aquifer (Table I). Total loss from the river during summer periods averaged 14% of upstream discharge. Summer upstream discharge (Q_{up}) exceeded downstream discharge (Q_{dn}) for all five rain-free periods examined. During spring, consistent gaining conditions prevailed despite a similar hydropeaking regime (Figure 3B). Integration across these 9 days in spring indicated average reach gains of 3.79 m^3/s. One suitable autumn analysis period was identified as well during which GW was close to zero. However, tributary discharge during this period was not directly measured and was likely well above levels at which our regression with the North River applies. Observation of persistent losing periods during summer periods suggests that some mechanism acting in concert with abrupt stage changes drives water permanently away from the river.

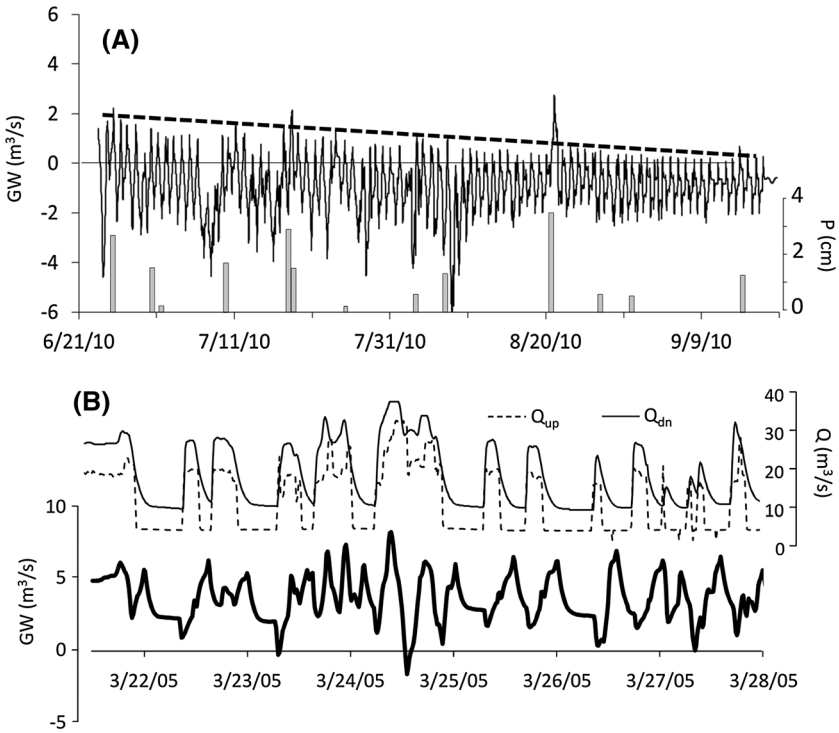

Figure 3. A 12-h moving average of the GW term from Equation (1) (A) shows a decline in the magnitude of temporary positive (gaining) excursions. Dashed dark line highlights this trend. Daily precipitation measured in Ashfield, MA depicted by grey bars. (B) Upstream and downstream discharge during spring 2005 hydropeaking with resultant GW term depicted with heavy black line. Q_{up} is lagged 4.5 h. Q_{up} for 2010 cannot be shown due to a confidentiality agreement signed with the data provider

Conservative error propagation, designed to minimize loss estimates, resulted in smaller losses from the river. However, Q_{up} still exceeded Q_{dn} for all evaluation periods. The downward revision of losses ranged from 0.06 to 0.41 m^3/s, for an average of 14% reduction in net losses (Supplementary Figure 3). Therefore, we can state without qualification that the river loses water consistently during summer.

A time series of the GW term of Equation (1) shows a clear negative trend in the magnitude of temporary gaining periods throughout summer of 2010 (Figure 3A). Short gaining periods occurred at the beginning of the low stage phase of each dam-induced hydrograph. As discussed earlier and noted by Gerecht *et al*. (2011), a dam-induced decrease in stage causes a local temporary head gradient reversal back towards the river. Sharp positive excursions from the seasonal decrease in the GW term are explained by precipitation events and accompanying runoff that was not accounted for in our four gauged tributaries. Lack of observations during high stage events on tributaries makes the magnitudes of these displayed hydrograph spikes uncertain due to error in tributary rating curves for high stage values.

Streambed observations

Streambed observations provide a more detailed perspective on the dynamics of SWGW interaction at sites with varying geologic context. Due to profound heterogeneities in streambed hydraulic conductivities at the pool and riffle scale (Conant, 2004) and sparse observations due to limited equipment, these data should be viewed primarily as confirmation of water budget observations made at the reach scale. Nevertheless, streambed temperature patterns generally confirmed losing conditions, especially during dam releases, with notable exceptions due to pool and riffle scale changes in valley morphology.

Site 1

Located just below the Fife Brook dam, this site is characterized by a bedrock bound channel with very limited transmissivity in the limited to non-existent riparian aquifer (Figure 4D). As a consequence of the minimal porous media and accompanying storage, changes in river stage quickly permeated the entirety of the narrow strip of bank alluvium. Thus, minimal gradient could be maintained between river head and that in the HZ (Figure 4A). The stage–VHG relationship was nearly horizontal indicating that regardless of changes in stage, VHG remained nearly absent.

Vertical temperature distribution at site 1 generally confirmed limited stage change-induced hyporheic pumping, consistent with the findings of Hanrahan (2008). Namely, the deepest temperature logger, at

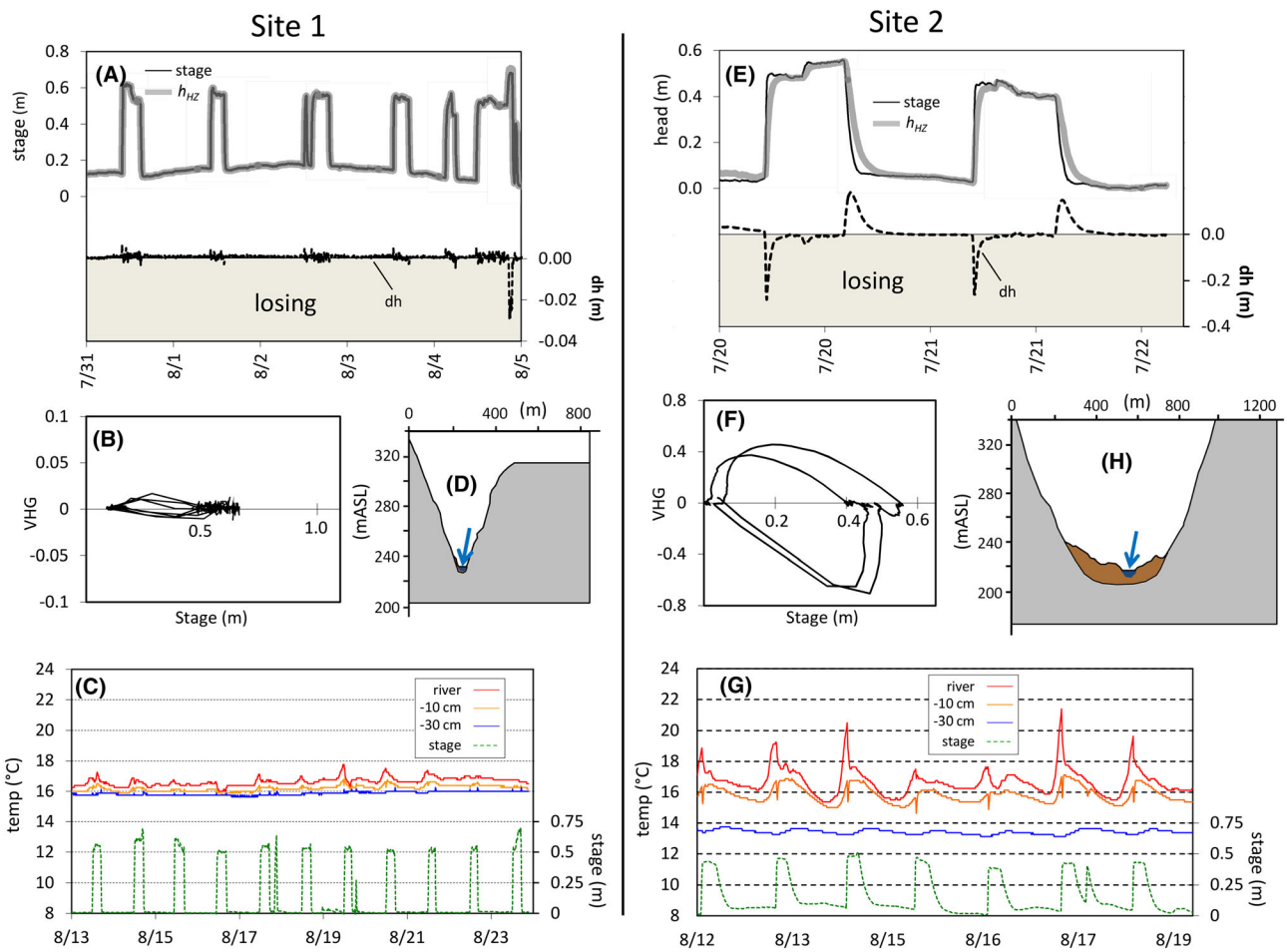

Figure 4. Streambed observations from site 1 (A–D) and site 2 (E–H). A and E show river stage, head 50 cm below the river bed (HZ Head), and the difference between these two measurements (dh); note that dh is plotted at different scales for sites 1 and 2. B and F show vertical hydraulic gradient (VHG) as a function of stage. C and G plot temperature in the river, as well as 10 cm and 30 cm into its bed. River stage depicted with green dashed line. D and H show schematic valley cross sections. Bedrock is shaded grey, valley fill is brown, and the river location is identified by a blue arrow

30 cm below the streambed, recorded almost no change in temperature regardless of changes in stage. Fife Brook Dam, Lower Bear Swamp Reservoir's bottom release dam, discharges cold water resulting in relatively steady river temperature and minimal diurnal temperature swings. HZ temperature 10 cm below the riverbed weakly echoed surface temperature signals. However, 30 cm into the HZ, temperature varied minimally above the resolution of the logging instrument. The continuous low temperature of the HZ here illustrates that insignificant volumes of slightly higher temperature river water are advected below the riverbed.

Site 2

At site 2, the river runs over a moderately wide (~200 m) valley bottom with up to 7-m-thick unconsolidated sediments (Figure 4H). It was expected that intermediate valley fill dimensions would provide for moderate SWGW exchange. With only seismic profiling and shallow auguring, we cannot be sure what comprises the roughly 7 m of sediments here. The VHG record suggests that the bank and HZ media impeded porous flow to a greater degree than sites 3 and 4. The low K here is evidenced by large dh values following abrupt stage changes (Figure 4E). The wide circle of the stage–VHG relationship suggests that gaining or losing conditions are highly hysteretic (Figure 4F), with the direction of flow highly dependent on previous stage. The near symmetry of the record about the *x*-axis indicates that the river here was neither strongly gaining nor losing over longer time periods.

The surface water diurnal temperature signal here appeared more like that of an unregulated river, with rising values during the morning hours due to heating that occurred in the 4 km downstream from Fife Brook Dam (Figure 4G). However, the daily arrival of the cold dam flood hydrograph from upstream ended morning increases in surface water temperature. Temperature 10 cm below the river bottom closely mirrored that at the surface, but

never exceeded it. As observed in streambed temperature records in Hatch *et al.* (2006) and other studies, the diurnal temperature signal at depth here lagged behind that at the surface due to the time for heat to reach that depth. At the deepest level, 30 cm, the diurnal signal is barely visible. The low temperature at this level approximates that of regional groundwater, suggesting that water from the river does not strongly influence temperature at depth.

Immediately following abrupt stage increases, we observed that the 10-cm temperature logger recorded a short-lived drop in temperature just as the river head increased (Figure 4G). We would otherwise expect surface water to be driven down and raise the HZ temperature. Boutt (2010) noted that loading of the riparian aquifer by added mass from the sudden arrival of a dam release flood wave could cause a jump in head in layers below confining units. If this process operates at site 2, one would expect a brief upward hydraulic gradient, pushing deeper, colder water towards the surface. Poroelastic loading driving colder water up explains this brief drop in temperature at depth when we would otherwise expect warming there. Furthermore, it indicates that a confining layer likely exists here close to the surface, consistent with the short duration of maintained VHG.

Sites 3 and 4

Sites 3 and 4 have similar valley geometries, similar hydrogeologic settings, and appear to respond similarly to abrupt stage increases (Figure 5). At both sites, wide and deep glaciofluvial deposits fill upwards of 40 m of over-deepened bedrock depression. Postglacial deposition of silty-fine to very fine sand underlies the streambed and grades finer downstream towards site 4. Coarse, high conductivity (up to 30 m/day) alluvium covers these deposits and forms the river banks in this reach. At both sites, referenced stage elevation exceeded HZ head at almost all times (Figure 7A, E) resulting in a negative VHG (Figure 5B, F). Immediately following flood-wave arrival, the difference in head was especially pronounced, when higher stage strongly drove water out of the river and into the riparian aquifer.

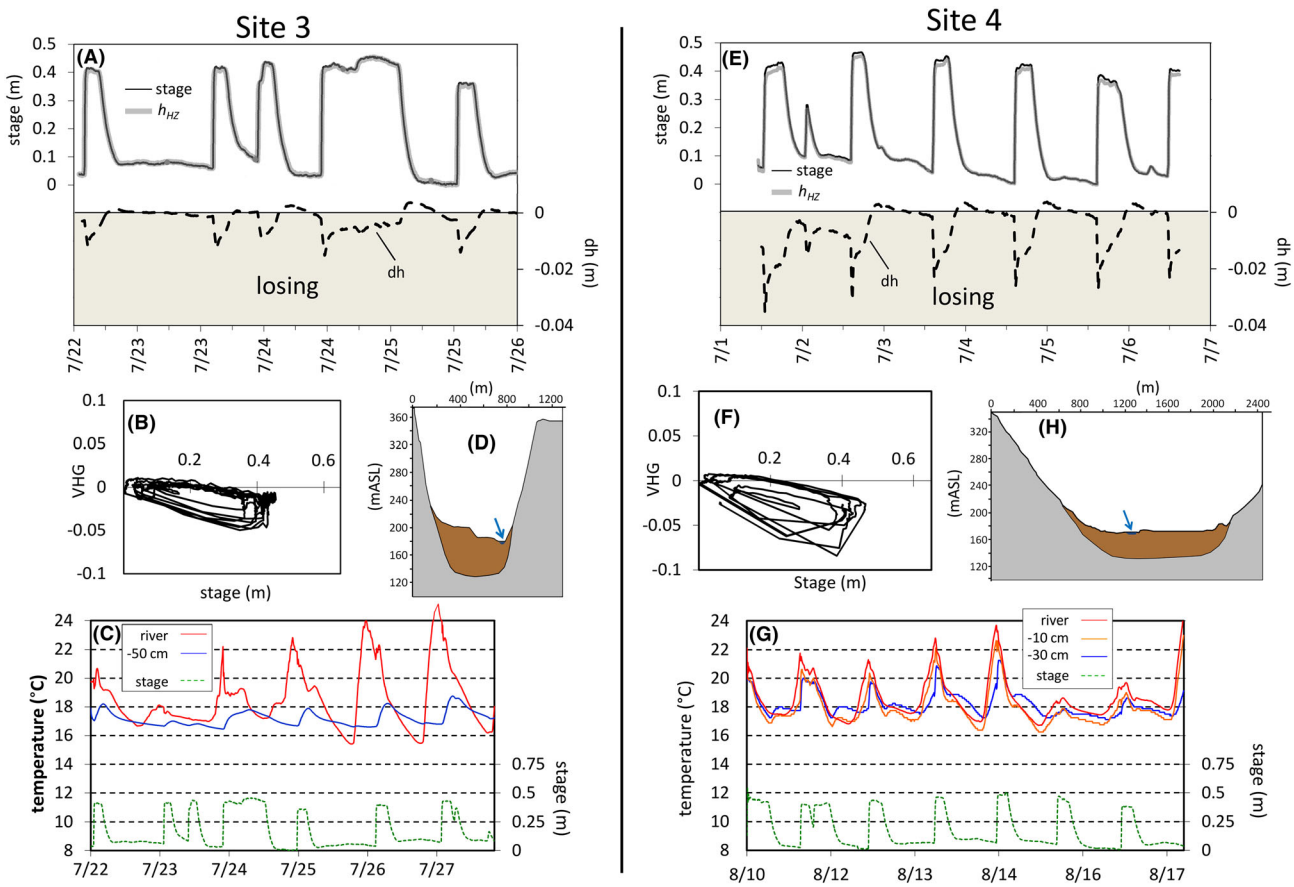

Figure 5. Streambed observations from site 3 (A–D) and site 4 (E–H). A and E show river stage, head 50 cm below the river bed (HZ Head), and the difference between these two measurements (dh). B and F show vertical hydraulic gradient (VHG) as a function of stage. C and G plot temperature in the river, as well as 10 cm and 30 cm into its bed. River stage is shown in green dashed line. D and H show schematic valley cross sections. Bedrock is shaded grey, valley fill is brown, and the river location is identified by a blue arrow

Both sites 3 and 4 display hysteretic VHG–stage curves (Figures 5B and 7F) that remain almost entirely below the *x*-axis. Daily dam releases, together with the influence of prior HZ head conditions on the direction of the VHG, caused this cyclic pattern in the VHG–stage relationship. For example, just before an abrupt stage increase, the hydraulic gradient between surface and HZ water was at its minimum. When the flood wave arrived, river head (h_R) jumped dramatically above HZ head (h_{HZ}), making the VHG strongly negative. The slow rise in h_{HZ} in response to downward seepage from the river reduced VHG, as indicated by the curve approaching the *x*-axis. When stage fell abruptly, h_{HZ} remained briefly elevated, causing the relationship to plot slightly above the *x*-axis and the river to gain back some of the lost water before the next flood wave arrived and forced more water into the subsurface.

At sites 3 and 4, most data points on the VHG–stage relationship (Figures 5B and 7F) fall below the *x*-axis, indicating that the river likely lost water at both locations. In general, the magnitude of VHG at site 4 was greater than that at site 3, perhaps reflecting the downstream decrease in grainsize which would cause a similar decrease in hydraulic conductivity and serve to better maintain a gradient during high stage events.

Streambed temperature records at sites 3 and 4 (Figures 5D and 7H) both show closely coupled stream and HZ temperatures. The added depth of the site 3 piezometer, which is shown in place of the faulty VTD probe data, caused expected additional dampening and lagging of the diurnal temperature signature.

Slug testing

Hydraulic conductivity (K) estimates for all sites are relatively high (>20 m/d) with values generally being higher at the two downstream sites (Table II). Results from site 3 vary considerably, possibly due to a poor connection between the piezometer and streambed media, allowing for a rapid attenuation of the initial head perturbation via short circuiting around the outside of the well bore. Due to the point-scale nature of these slug test-based K estimates, results are presented with the caveat that they do not capture the spatial heterogeneity at each site. Rather, they provide some context for observed changes in hyporheic head within each piezometer.

Riparian aquifer wells

Streambank head observations from Friesz (1996) corroborate strongly losing conditions at this location. In the well located 3 m away from the river and screened within the high horizontal hydraulic conductivity alluvium at site 4, head was consistently higher than that observed in the well 40 m away from the river. Observations taken over 14 days in early July indicate an average difference in head of 0.11 m corresponding to an average head gradient of 0.0028 away from the river (Figure 6). Our Darcy-based approach, when applied to both banks of the 19.5-km river reach, results in an average loss of 3.6 m^3/s, or roughly three times water budget losses reported in Table I.

Table II. Slug test results from DFR sites 1–4 reported in m/d. Results from site 3 vary considerably due to a poor connection between the piezometer and streambed media, allowing for a rapid attenuation of the initial head perturbation

Site	1	2	3	4
Trial 1 (m/d)	14.1	35.0	353.5	142.6
Trial 2 (m/d)	23.7	36.6	126.4	138.2
Trial 3 (m/d)	23.6	33.7	288.3	108.9
Average (m/d)	20.5	35.1	256.1	130.5

Additional observations

Due to problems with piezometer screen clogging and infrequent hydropeaking during piezometer deployment, data from site 5 are less valuable than sites 1 – 4. Streambed temperature and VHG data from that site generally indicated gaining conditions, which is consistent with limited depth to bedrock and pinching out of the alluvial basin material at the site driving groundwater to the surface from basin-scale flowpaths.

DISCUSSION

Our water budget approach to understanding the effects of hydropeaking on SWGW interactions suggests that the DFR study reach loses water as a result of hydroelectric management practices. Given the combination

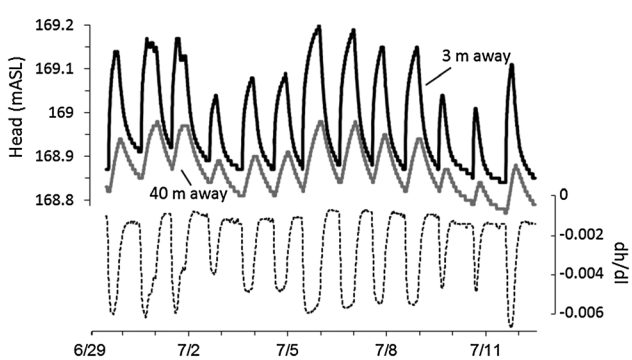

Figure 6. Head observations at site 4 in wells screened in riverbank alluvium at distances of 3 m from the river (black line) and at 40 m from the river (grey line). Head gradient (dh/dl) time series is plotted below head observations with dashed line. Data taken from Friesz (1996)

of New England's temperate climate and the reach's expansive till-mantled upland watershed draining towards the valley fill aquifer, one would expect the water table to slope towards the river and drive water there. Comparison with the adjacent and geomorphically similar, but minimally regulated Westfield River (WFR) watershed, illustrates the impact of upstream storage on summer flows in the DFR. The DFR's July and August 2010 discharge exceeds the WFR's by 67%, despite having a 27% smaller watershed study area.

Juxtaposition of a relatively smaller watershed and larger discharge shows the extent to which the DFR's average summer stage is elevated by releases from upstream reservoir storage, thereby affecting the gradient across the SWGW exchange zone. Whereas DFR water budget accounting shows consistently decreasing downstream flow, WFR discharge increased by an average of 72% in a 28-km reach between the confluence of its three main tributaries and its downstream gauge during July and August 2010 (Figure 7A). Although this increase was due in part to tributaries entering the WFR, its watershed area only increases by 61%, smaller than the increase in discharge. In this humid region, it is reasonable to deduce that the proportional increase is due in part to groundwater inputs. The same analysis on the DFR study reach shows that over the course of the summer, there is only a 1% increase in downstream discharge, despite the contributing area increasing by 40% down the 19.5-km study reach. Upstream storage roughly doubles DFR area normalized discharge during summer relative to that of the WFR (Figure 7B).

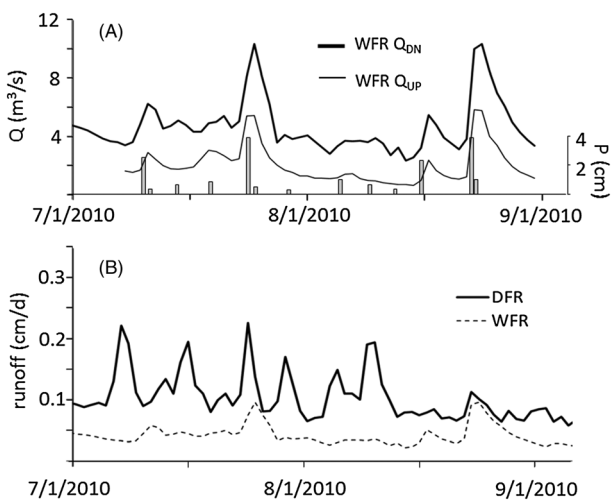

Figure 7. (A) Upstream and downstream daily average discharge for the Westfield River, not accounting for tributary inputs within the interim river reach. Note that discharge increases in the downstream direction at all times. Daily precipitation in Huntington, MA depicted by grey bars. (B) Average daily runoff from Deerfield (DFR) and Westfield (WFR) Rivers. The DFR record always exceeds the WFR record during summer despite smaller watershed area

An argument could be made that downstream change in the DFR's geomorphic confinement may in itself cause losses to the groundwater system. However, the WFR study reach lies within a similar geomorphic context and contains similar changes in confinement. More specifically, within its study reach, the DFR upper 10 km averages 80 m of riparian aquifer width, broadening to an average of 430 m in the reach's lower half. Similarly, the WFR expands from an average riparian aquifer width of 90 m in its upper 13 km to 570 m in its lower half (Supplementary Figure 4). Furthermore, the downstream end of the DFR study reach is defined by a pinching out of the riparian aquifer as bedrock comes to the surface in the vicinity of the downstream gauge (Q_{dn}). Water lost to the riparian aquifer as a result of reduced river confinement should therefore return within the study reach.

Two possible mechanisms may explain permanent losses from the river: (1) stage increases drive water into groundwater storage at time scales exceeding seasonal cycles; (2) transpiration by riparian vegetation removes water from the aquifer allowing for repeated losses. The first mechanism seems unfeasible given that empty pore spaces would quickly be filled given the volume of water being lost from the river. Correlation between the amount of loss for individual flood events and several independent variables was tested. The variables tested were: (A) the magnitude of the stage change for an individual event; (B) the duration of the elevated stage event; and (C) evaporative flux from the river as a proxy for potential evapotranspiration (PET) by riparian vegetation.

It was initially hypothesized that a higher hydraulic gradient away from the river caused by a larger dam release would drive more water into the riparian aquifer and therefore correlate well with reach-scale loss. However, no correlation was observed between changes in discharge from before to during a dam release and the amount of loss for that release. This is likely due to the small variation in the stage difference during hydropeaking. For example, at site 3, the change in stage in response to a dam release ranged from a minimum of 36 cm to a maximum change of 42 cm.

The duration of high discharge events varied a great deal from as short as 7 h to as long as 24 h. It was hypothesized that a longer period of time during which high stage caused a hydraulic gradient away from the river would drive more water out of the river. Two events extending well into the following calendar day were considered outliers and discarded. Duration of dam release *versus* reach-scale loss was plotted for the remaining events for 2010 rain-free periods. A cluster of data points around 7.5 h with no visible trend indicated that flood duration did not adequately explain the variation in the amount of loss for a given event (Figure 8A).

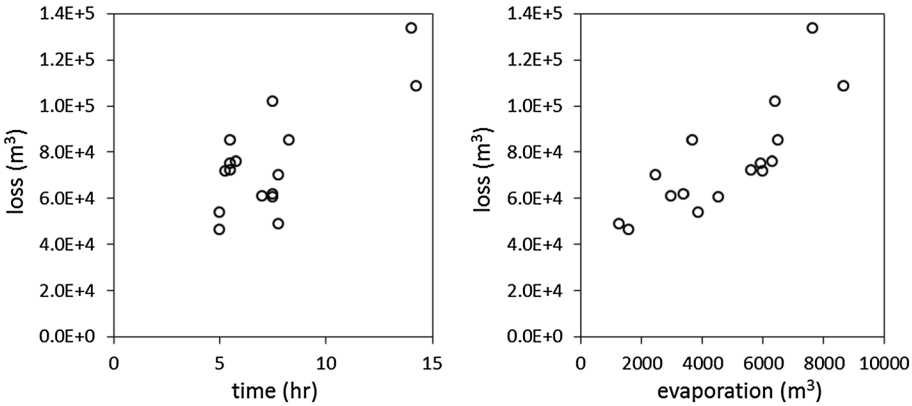

Figure 8. (A) Duration of dam release and (B) volumetric evaporation from the river surface both plotted against total water loss (GW term in Equation (1)) for individual dam release events in 2010

Last, ET from riparian vegetation was invoked to explain persistent losses throughout the summer. Because vegetative transpiration data were not available, direct evaporation from the DFR study reach surface was used as a proxy for ET forcing. Generally shallow water tables in the riparian zone, bolstered by daily bank storage events, make it likely that riparian vegetation exists in an energy, rather than moisture-limited growing regime. Therefore, evaporation from an open water surface calculated using an available energy balance method such as Penman (1948) provides an approximation for ET forcing from riparian forests. Although evaporation rate did not correlate well with total reach-scale loss, total estimated volumetric evaporation from the study reach displayed a strong relationship (Pearson $r^2 = 0.65$, $p = 0.016$) with reach loss (Figure 8B).

Total volumetric evaporation calculated as the product of linear evaporation rate, area of the study reach, and duration of the flood proved to be a better causal variable for two reasons: (1) total evaporation factored in the effects of evaporative forcing as well as the duration of the event—a longer event would permit more evaporation to occur—and (2) removal of water from the riparian aquifer was necessary to explain persistent and increasing losses throughout the summer. Thus, volumetric evaporation was really an incorporator of natural evaporative variables and human-controlled flood duration.

Previous temperate climate studies have documented the effects of riparian vegetation ET on both low-order streams (Gribovszki *et al.*, 2008) and large alluvial plain systems (Krause and Bronstert, 2007). The significant role of ET suggested by this study on a large, hydropeaking river's in-stream flows, however, is undocumented. Comparison with the Westfield River suggests that hydropeaking is likely responsible for the losses from the DFR and correlation with evaporative forcing. Daily bank-full events on the DFR raise the water table adjacent to the river (Figure 9D). This in turn drives the capillary fringe higher allowing more vegetation to access water that otherwise would have returned to comprise part of the river's low stage discharge.

Over the course of each anthropogenic flood, the pressure wave propagates into the bank causing pore spaces immediately above the capillary fringe fill due to matric suction. Suction is sustained all summer by the cumulative effect of ET, which generally maintains an upward gradient towards the root zone. Therefore, via hydropeaking, water availability in the riparian zone adjacent to these artificially high stage events can shift ET from a moisture-limited towards an energy-limited phenomenon. Each day's bank vegetation transpiration serves to maintain or intensify this gradient, sucking water away from the river. ET from preceding days may play a role in the amount of loss for a given flood event due to its role removing water from the oscillating capillary fringe zone.

Focusing in from reach-scale data to discrete piezometers and streambed thermistors indicates that valley width plays a large role in determining the magnitude of SWGW exchange and therefore potential water loss due to hydropeaking. Streambed temperature data from wider valley bottom sections (sites 3 and 4) illustrate enhanced hyporheic pumping where extensive porous media extend laterally great distances away from the river providing bank storage during short-lived hydroelectric floods.

Riparian head observations that indicated 2–3 times greater losses than those observed by water budget methods are consistent with this influence of reach morphology on the magnitude of losses. Because we have applied this exercise to the site with the most transmissive (wide and high K) valley aquifer, this number by no means approximates processes as they operate in the field. Rather it serves to highlight that (a) this river is indeed strongly losing and (b) that losses are concentrated in wide valley bottoms where hyporheic pumping extends far from the river, thus explaining the discrepancy with water budget calculations.

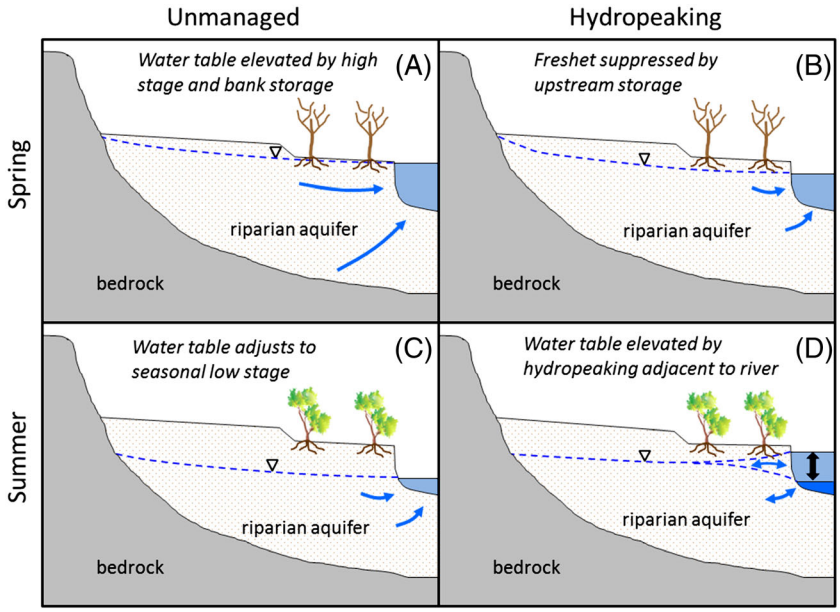

Figure 9. Schematic cross-sectional illustrations of how seasonal changes affect unmanaged *versus* hydropeaking river reaches. The water table is depicted by dashed blue line. The river is at right in each image. Blue arrows depict magnitude and direction of groundwater flow. Note that hydropeaking can make river water available to transpiring trees on lower terraces, whereas those along unmanaged streams are hydraulically disconnected from the saturated zone during summer

A time series of the GW term of Equation (1) (Figure 3A) shows the cumulative effect of ET over the course of the summer. As the riparian aquifer is drawn progressively down by the seasonal effect of ET, the magnitude of brief, low-stage gaining periods decreases. By the end of summer, the river loses water almost continuously, even during low-stage events. Three factors cause a hydraulic gradient away from the river and make it nearly impossible for the river to gain even after dam release events. First, upstream storage allows for daily bank-full events, which cause a mounding of the water table similar to snowmelt-fed streams in arid regions. Second, the cumulative effect of vegetative transpiration progressively removes water from the vadose zone, thereby increasing matric suction and removing water from the saturated zone and depressing the water table. Last, and unique to dam-controlled rivers, storage and suppression of the spring hydrograph in upstream reservoirs artificially subdue expected increases in riparian aquifer head during the spring (Figure 9B). Analysis of 2000–2005 upstream reservoir storage volume time series indicates an average capture of 7.7e10 m^3 from March to May, which would equate to an increase in average spring discharge of 12.23 m^3/s if allowed to flow downstream during the spring. Krause and Bronstert (2007) showed that in higher order streams, surface water–groundwater dynamics play a larger role in changes in riparian aquifer head than direct precipitation inputs. Whereas most valleys experience a significant freshet during which high river stage induces bank storage and raises the riparian water table, the DFR begins summer already at a deficit because the freshet is dampened by upstream storage (Figure 9B).

If hydropeaking indeed can induce a typically gaining river reach to lose water permanently, dam operators face a whole new set of considerations when drafting dam-release procedures. From an ecological standpoint, these results may be heartening, at least early in the growing season. Short-term bank-storage from previous releases may bolster minimum flows via the return flow of bank storage from previous dam releases. While increasing the total volume of low flows, this riparian zone return water also provides thermal buffering due to its relatively lower temperature. However, during late summer, when coldwater fisheries are most vulnerable, broader seasonal drawdown of the riparian aquifer would negate this benefit due to reversal of the hydraulic gradient away from the river at nearly all times in the flood cycle. The combination of hydropeaking and resultant water table mounding adjacent to dam controlled rivers may mean that even in humid areas, licensed minimum flow requirements may be insufficient to meet desired goals if substantial losses occur within the reach of concern.

Recognition of hydropeaking-induced losses should also inform hydropower optimization techniques. Rivers used for hydropower production often flow through a series of run-of-river generating facilities downstream of major storage impoundments. Currently, energy producers account for water mass conservatively and plan schedules to make use of each unit of water at subsequent downstream dams (De Ladurantaye *et al.*, 2007). In deregulated energy markets, optimization techniques tend

to favour larger releases on days with greater demand and therefore higher energy prices (Shawwash, Siu and Russell, 2000). However, in light of the finding that during the growing season up to 10% of this water may disappear from the system for every 20 km it travels, it might be prudent to mitigate hydropeaking in certain contexts to thereby reduce water losses.

In river systems where multiple dams in series transform energy from the same water into electricity at successive downstream facilities, recognition of induced losses from hydropeaking may significantly alter best practices. Changes to optimization methods will depend on downstream geomorphic conditions, regional flood threat, head-drop at various facilities, and other factors. Constrained river systems with bedrock channels will likely see little loss if the interpretation about riparian vegetation above holds true. Nevertheless, hydroelectric operators in most watersheds face an unforeseen tradeoff to making large releases on hot days with high evaporative demand.

CONCLUSION

Water budget analysis shows incontrovertibly that the DFR study reach loses water, whereas a non-hydropeaking geomorphically similar reference stream (Westfield River) does not. While this comparison with a neighbouring river is sound, and a qualitative mechanistic description of hydropeaking-induced losses is highly plausible, it remains to be seen if river management for hydropower causes losses on other systems. Observations of vertical hydraulic gradient and streambed temperatures generally support water budget findings and show that induced water losses are greater in reaches with broad alluvial aquifers in contact with the river. Cross correlations with reach losses suggest that the duration of high stage events and the amount of evaporative forcing explain in part the cause of river losses. Limited far-field piezometric data within the riparian aquifer and a lack of direct observation of evapotranspiration make it hard to constrain the amount of loss due to SWGW interactions and riparian vegetation dynamics. However, a multiple scale approach using both reach scale water budget accounting and point measurements of SWGW interactions offers a unique perspective on how hydropeaking can cause a typically gaining river reach to lose water.

ACKNOWLEDGEMENTS

We gratefully acknowledge support from the National Institutes for Water Resources via the Massachusetts Water Resources Research Center. Taylor Lucey assisted with field data collection. Steven Sauter of Ashfield, MA generously provided weather data for evaporation estimates. Peer review by Audrey Sawyer and two anonymous reviewers greatly improved this manuscript.

REFERENCES

Arntzen EV, Geist DR, Dresel PE. 2006. Effects of fluctuating river flow on groundwater/surface water mixing in the hyporheic zone of a regulated, large cobble bed river. *River Research and Applications* **22**(8): 937–946. DOI: 10.1002/rra.947

Boulton AJ, Datry T, Kasahara T, Mutz M, Stanford JA. 2010. Ecology and management of the hyporheic zone: stream–groundwater interactions of running waters and their floodplains. *Journal of the North American Benthological Society* **29**(1): 26–40. DOI: 10.1899/08-017.1

Boutt DF. 2010. Poroelastic loading of an aquifer due to upstream dam releases. *Ground Water* **48**(4): 580–592. DOI: 10.1111/j.1745-6584.2009.00663.x

Boutt DF, Fleming BJ. 2009. Implications of anthropogenic river stage fluctuations on mass transport in a valley fill aquifer. *Water Resources Research* **45**. DOI: 10.1029/2007WR006526.

Bouwer H, Rice RC. 1976. A slug test method for determining hydraulic conductivity of unconfined aquifers with completely or partially penetrating wells. *Water Resources Research* **12**(3): 423–428. DOI: 10.1029/WR012i003p00423

Brunke M, Gonser T. 1997. The ecological significance of exchange processes between rivers and groundwater. *Freshwater Biology* **37**(1): 1–33.

Cardenas, MB. 2010. Thermal skin effect of pipes in streambeds and its implications on groundwater flux estimation using diurnal temperature signals. *Water Resources Research* **46**(3). DOI: 10.1029/2009WR008528

Conant, B. 2004. Delineating and quantifying ground water discharge zones using streambed temperatures. *Ground Water* **42**(2): 243–257.

De Ladurantaye D, Gendreau M, Potvin JY. 2007. Optimizing profits from hydroelectricity production. *Computers & Operations Research* **36**(2): 499–529. DOI:10.1016/j.cor.2007.10.012

Findlay S, Strayer D, Goumbala C, Gould K. 1993. Metabolism of streamwater dissolved organic carbon in the shallow hyporheic zone. *Limnology and Oceanography* **38**(7): 1493–1499. DOI: 10.4319/lo.1993.38.7.1493

Friesz PJ. 1996. Geohydrology of Stratified drift and streamflow in the Deerfield River Basin, Northwestern Massachusetts. Water-resources investigations report 96-4115. US Department of the Interior, US Geological Survey.

Gerecht KE, Cardenas MB, Guswa AJ, Sawyer AH, Nowinski JD, Swanson TE. 2011. Dynamics of hyporheic flow and heat transport across a bed-to-bank continuum in a large regulated river. *Water Resources Research* **47**(3): DOI: 10.1029/2010WR009794

Graf WL. 1999. Dam nation: a geographic census of American dams and their large-scale hydrologic impacts. *Water Resources Research* **35**(4): 1305–1311.

Gribovszki Z, Kalicz P, Szilágyi J, Kucsara M. 2008. Riparian zone evapotranspiration estimation from diurnal groundwater level fluctuations. *Journal of Hydrology* **349**(1): 6–17. DOI: 10.1016/j.jhydrol.2007.10.049

Hanrahan TP. 2008. Effects of river discharge on hyporheic exchange flows in salmon spawning areas of a large gravel-bed river. *Hydrological Processes* **22**(1): 127–141. DOI: 10.1002/hyp.6605

Hatch C0E, Fisher AT, Revenaugh JS, Constantz J, Ruehl C. 2006. Quantifying surface water–groundwater interactions using time series analysis of streambed thermal records: method development. *Water Resources Research* **42**(10). DOI: 10.1029/2005WR004787

Jones JB, Fisher SG, Grimm NB. 1995. Nitrification in the hyporheic zone of a desert stream ecosystem. *Journal of the North American Benthological Society* **14**: 249–258. DOI: 10.2307/1467777

Koteff C, Pessl Jr F. 1981. Systematic ice retreat in New England. US Geological Survey Professional Paper 1179.

Krause S, Bronstert A. 2007. The impact of groundwater–surface water interactions on the water balance of a mesoscale lowland river catchment in northeastern Germany. *Hydrological Processes* **21**(2): 169–184. DOI: 10.1016/j.jhydrol.2007.09.028

Ligon FK, Dietrich WE, Trush WJ. 1995. Downstream ecological effects of dams. *BioScience* **45**(3): 183–192. DOI: 10.2307/1312557

Mabee S, Fleming B, Boutt D. 2007. Hydrogeologic assessment of the West Charlemont aquifer, project completion report. *Charlemont: Massachusetts,USA*.

Magilligan FJ, Nislow KH, Graber BE. 2003. Scale-independent assessment of discharge reduction and riparian disconnectivity following flow regulation by dams. *Geology* **31**(7): 569–572. DOI: 10.1130/0091-7613(2003)031<0569:SAODRA>2.0.CO;2

Mulholland PJ, Marzolf ER, Webster JR, Hart DR, Hendricks SP. 1997. Evidence that hyporheic zones increase heterotrophic metabolism and phosphorus uptake in forest streams. *Limnology and Oceanography* **42**(3): 443–451. DOI: 10.4319/lo.1997.42.3.0443

Penman HL. 1948. Natural evaporation from open water, bare soil and grass. *Proceedings of the Royal Society of London. Series A. Mathematical and Physical Sciences* **193**(1032): 120–145. DOI: 10.1098/rspa.1948.0037

Poff NL, Allan JD, Bain MB, Karr JR, Prestegaard KL, Richter BD, Sparks RE. Stromberg JC. 1997. The natural flow regime. *BioScience* **47**(11): 769–784. DOI: 10.2307/1313099

Raymond HL. 1979. Effects of dams and impoundments on migrations of juvenile chinook salmon and steelhead from the snake river, 1966 to 1975. *Transactions of the American Fisheries Society* **108**(6): 505–529.

Sawyer A, Bayani Cardenas M, Bomar A, Mackey M. 2009. Impact of dam operations on hyporheic exchange in the riparian zone of a regulated river. *Hydrological Processes* **23**(15): 2129–2137. DOI: 10.1002/hyp.7324

Shawwash ZK, Siu TK, Russell SD. 2000. The BC hydro short term hydro scheduling optimization model. *IEEE Transactions on Power Systems* **15**(3): 1125–1131.

Valiantzas JD. 2006. Simplified versions for the penman evaporation equation using routine weather data. *Journal of Hydrology* **331**(3–4): 690–702. DOI: 10.1016/j.jhydrol.2006.06.012

Ward JV, Stanford JA. 1983. The serial discontinuity concept of lotic ecosystems. *Dynamics of Lotic Ecosystems* **10**: 29–42.

SUPPORTING INFORMATION

Additional supporting information may be found in the online version of this article at the publisher's web-site.

